RF Optics Study for DSS-43 Ultracone Implementation

P. Lee and W. Veruttipong
Ground Antennas and Facilities Engineering Section

The Ultracone feed system will be implemented on DSS 43 to support the S-band (2.3 GHz) Galileo contingency mission. The feed system will be installed in the host country's cone, which is normally used for radio astronomy, VLBI, and holography. The design must retain existing radio-astronomy capabilities, which could be impaired by shadowing from the large S-band feed horn. Computer calculations were completed to estimate system performance and shadowing effects for various configurations of the host country's cone feed systems. Also, the DSS-43 system performance using higher gain S-band horns was analyzed. A new S-band horn design with improved return loss and cross-polarization characteristics is presented.

I. Introduction

The Ultracone is an ultralow-noise S-band (2.3-GHz) feed system that will be implemented on DSS 43, the 70-m DSN antenna in Australia, for the Galileo S-band contingency mission. The Ultracone will have better performance than the S-band polarization diverse (SPD) design that is currently installed on DSS 43, allowing for higher data transmission rates from the Galileo low-gain S-band antenna. The performance improvements are achieved by making the Ultracone a receive-only, fixed-polarization system with copper components. The SPD design is a transmit-and-receive, polarization-diverse system. The Ultracone is predicted to lower the system noise temperature by 2.5 to 3.0 K. The requirements for the design are a maximum system noise temperature of 12.5 K at zenith and a minimum antenna and microwave gain of 63.3 dBi at a 45-deg elevation, referenced to the maser input flange.[1]

The Ultracone will be installed in the DSS-43 host country's cone. This cone is used primarily by radio astronomy, VLBI, and holography. The Ultracone feed system cannot easily be added without interfering with the already existing feed systems. One of the Ultracone task's functional requirements is to retain existing host country radio-astronomy capabilities. This article presents the RF optics study that examined options for implementing the Ultracone feed system without impacting radio-astronomy capabilities, while giving the best S-band performance possible.

[1] *Galileo S-Band Level C Review* (internal document), Jet Propulsion Laboratory, Pasadena, California, December 1992.

II. 70-m Antenna Geometry

The DSS-43 70-m antenna geometry is shown in Fig. 1.[2] The antenna has a symmetric main reflector and an asymmetric subreflector, which can be set only at discrete azimuthal stops. The reflector system focuses to a ring slightly above the top of three feed cones, which house the feed systems. Located on the focal ring are points that correspond to the subreflector stops. The phase centers of the feed systems are positioned at these focus points. Figure 2 shows a top view of the host country's cone that will be used to house the Ultracone feed system. It contains three focal points. F1 is the proposed location of the Ultracone, the radio-astronomy 22-GHz dual-feed system is currently located at F2, and F3 is used for radio astronomy, VLBI, and holography.

III. Improving S-Band Performance

A. Feed Horn Gain

The 70-m antenna optics were designed for the maximum gain-to-noise-temperature ratio (G/T) at 8.45 GHz using a 22.5-dBi feed horn.[3] For the original implementation of 2.295 GHz on the 70-m antennas, a 22.5-dBi horn was also used. At 2.295 GHz, the rear spillover past the main reflector is higher than at 8.45 GHz since the longer wavelength has a wider diffraction pattern off the subreflector. In a low-temperature system, such as the Ultracone, this spillover is a major contributor to the overall noise temperature. One method of reducing the rear spillover is to use a higher gain S-band feed horn.

The effects of increasing the horn gain were analyzed using JPL physical optics (P.O.) computer programs.[4] Increasing the horn gain to 23.1 dBi was found to reduce the rear spillover by about one-half, while only slightly decreasing the overall gain of the antenna. The horn gain was increased by adding an extension 26 cm long, which increases the aperture diameter from 66.2 to 72.3 cm. The G/T improvement is about 0.11 dB/K at 30-deg elevation, 0.14 dB/K at 45-deg elevation, and 0.23 dB/K at 90-deg elevation. Figure 3 shows the antenna performance versus horn aperture diameter at 2.295 GHz, and Tables 1 and 2 show the overall gain and noise temperature budgets with the 22.5-dBi and 23.1-dBi horns, respectively.[5] The G/T performance at 22 GHz was also analyzed using higher gain horns. Since the rear spillover past the main reflector is already very low at 22 GHz, the improvement in noise temperature is very slight. The resulting decrease in system gain, due to underillumination of the main reflector, offsets the improvement in noise temperature, causing the overall G/T to decrease.

B. New Horn Design

To further improve system performance at S-band, the feed horn was redesigned for better return loss and cross-polarization characteristics. Computer analysis of the new design predicts better than a −39-dB return loss over the transmit band (2.025 to 2.210 GHz) and receive band (2.2 to 2.3 GHz), compared to a −31- to −41-dB return loss over the same bands for the JPL standard S-band horn design.[6] The maximum predicted peak cross-polarization level is better than −40 dB for the new design, compared to −35 dB for the standard design. Figure 4 shows the computer-predicted return loss and cross-polarization levels for the new horn and the standard horn.

---

[2] A. G. Cha, *Physical Optics Analysis of NASA/JPL Deep Space 70-m Antennas*, JPL D-1853 (internal document), Jet Propulsion Laboratory, Pasadena, California, November 1984.

[3] W. F. Williams, *Considerations for Determining the Shaped Main Reflector for the DSN 70-Meter Upgrade Program*, JPL D-1875 (internal document), Jet Propulsion Laboratory, Pasadena, California, November 1, 1984.

[4] R. E. Hodges and W. A. Imbriale, *Computer Program POMESH for Diffraction Analysis of Reflector Antennas* (internal document), Jet Propulsion Laboratory, Pasadena, California, February 1992.

[5] D. Trowbridge and S. Petty, personal communication, Radio Frequency and Microwave Subsystems Section, Jet Propulsion Laboratory, Pasadena, California, August 5, 1994.

[6] "Horn Assy, Wide Band, Dual Mode," JPL Drawing 9449420, Rev. E (internal document), Jet Propulsion Laboratory, Pasadena, California, March 29, 1979.

The gain of the new horn is 23.1 dB at 2.295 GHz. Removing the final section of the horn results in a gain of 22.5 dB at 2.295 GHz, making it compatible with the standard S-band horn gain. Theoretical and measured far-field copolarization patterns are shown in Fig. 5 at 2.295 GHz in the receive band and at 2.025 GHz in the transmit band. The measured patterns were taken on a far-field range on the mesa at JPL. The theoretical patterns were calculated using a circular waveguide mode-matching program, CWG.F [1,2], and a circular-aperture far-field radiation program, CRAD.F [3].

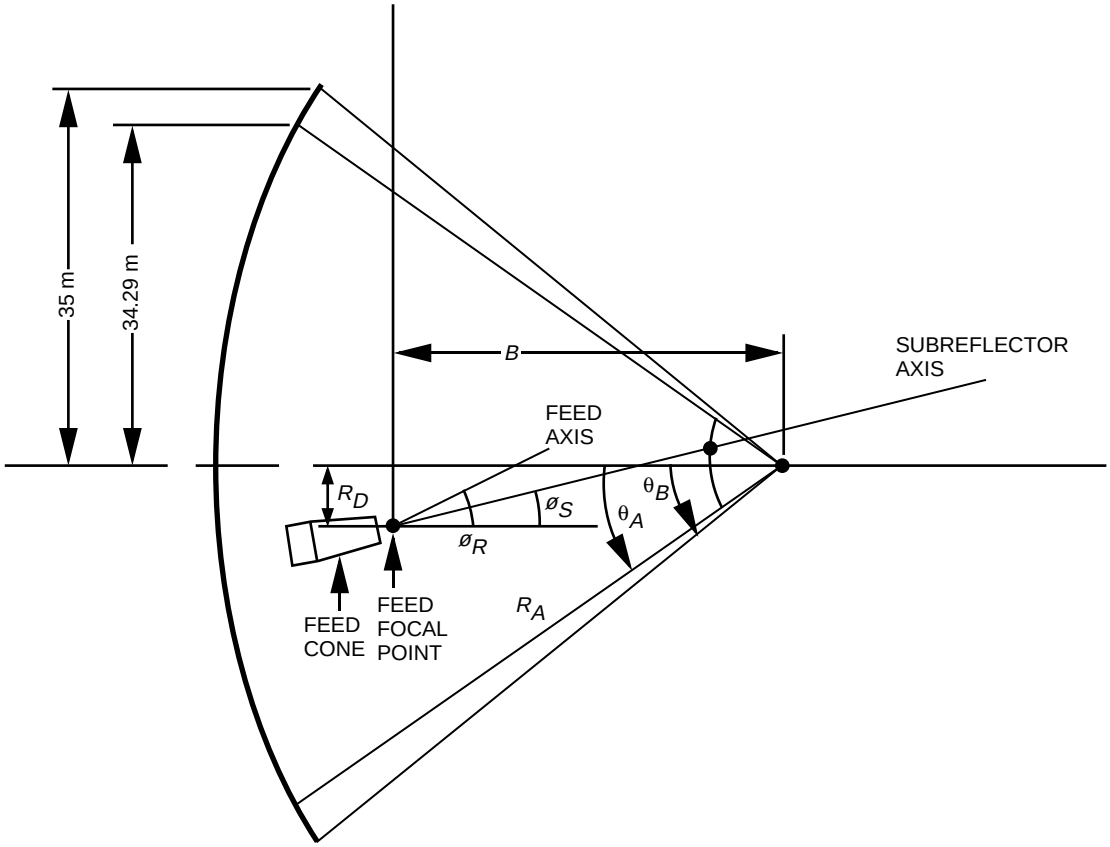

B = 15.451 m

R_D = 108.01 cm

ϕ_R = 5.73722 deg: ACTUAL FEED TILT FROM MAIN REFLECTOR AXIS, PRESENT TRICONE FEED

ϕ_S = 5.26000 deg: FEED TILT AT WHICH SUBREFLECTOR EDGE WOULD SUBTEND EQUAL ANGLES AT FEED PHASE CENTER, DEFINED AS SUBREFLECTOR OR AXIS FOR FABRICATION

θ_A = 62.2626 deg: (TO 34.29-m OPTICAL BOUNDARY)

θ_B = 63.31 deg: (TO 35 m)

R_A = 38.74 m

Fig. 1. DSS-43 70-m antenna geometry.

Two major design changes were made between the standard S-band horn and the new Ultracone horn. First, the corrugations were oriented perpendicular to the axis of the horn instead of perpendicular to the sidewall (Fig. 6). The JPL computer program used to analyze the horn (CWG.F) is a circular-waveguide mode-matching program. It can model the type of corrugations in the new horn design exactly, but can

only approximate the corrugations in the older design. It has been shown [4] that horns with either type of corrugations perform well. The orientation has little effect on fabrication costs.

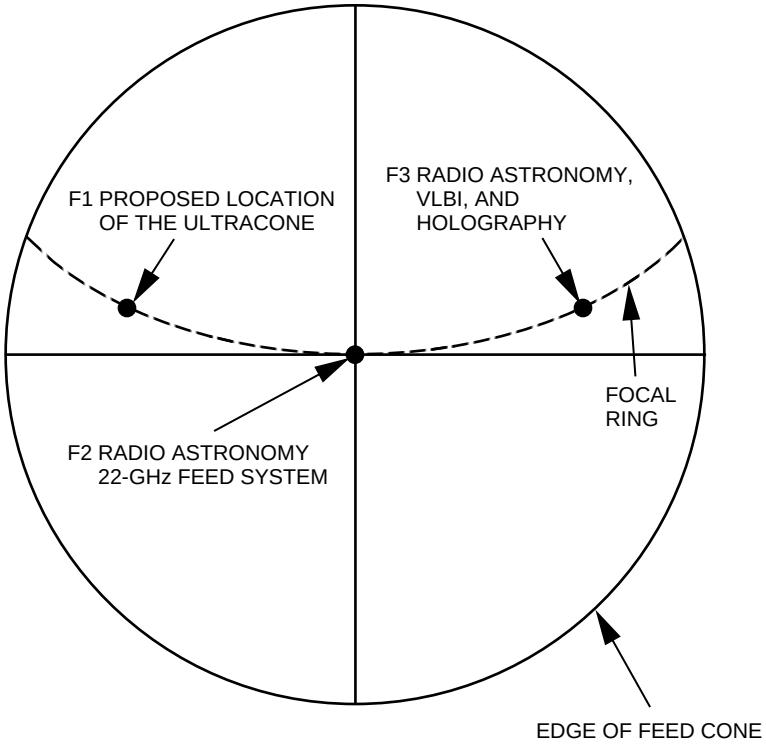

Fig. 2. Top view of DSS-43 host country's feed cone.

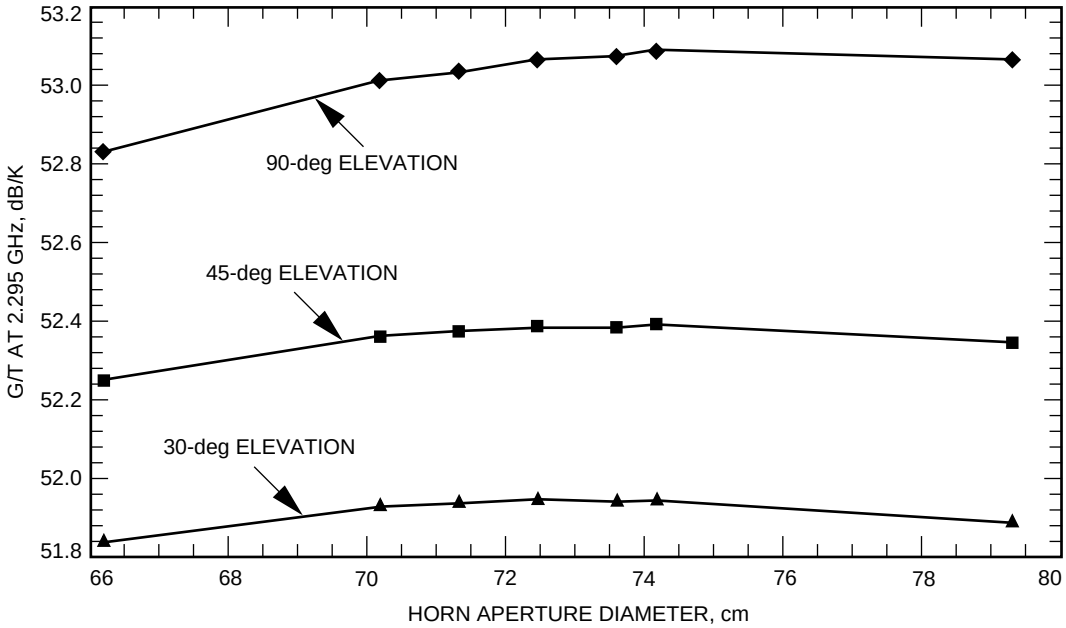

Fig. 3. DSS-43 G/T versus feed-horn aperture diameter at 2.295 GHz.

Table 1. Gain and noise temperature budgets at 2.295 GHz for a 22.5-dBi horn.

Noise temperature budget				
Element	Noise temperature, K			Comments
	90 deg	45 deg	30 deg	
Cosmic background	2.7	2.7	2.7	Effective black body
Atmosphere	1.9	2.6	3.6	
Subreflector forward spillover	0	0	0	
Main reflector rear spillover	1.42	1.07	0.96	240 K, 0.59 percent
Main reflector resistive	0.08	0.08	0.08	
Main reflector gap leakage	0.1	0.1	0.1	
Subreflector resistive	0.07	0.07	0.07	
Quadripod scatter	2.3	3.8	4.2	
Subtotal	8.57	10.42	11.71	Noise at feed aperture
Modified subtotal	8.53	10.38	11.66	Noise at preamplifier input −0.01855 dB at 20 deg C
Waveguide resistive	1.25	1.25	1.25	
Coupler injection	0.093	0.093	0.093	
Low-noise amplifier	2.036	2.036	2.036	
Follow up	0.037	0.037	0.037	
Total noise temperature	11.94	13.79	15.07	

Gain budget				
Element	Efficiency			Comments
	90 deg	45 deg	30 deg	
P.O. computed subtotal	0.90212	0.91003	0.90485	Includes F1 field: Forward spill: 0.9636 Rear spill: 0.9941 Central blockage: 0.988
Main reflector resistive	0.99977	0.99977	0.99977	
Main reflector panel leakage	1	1	1	Calculated
Main reflector gap leakage	1	1	1	Calculated
Main reflector surface rms	0.997	0.997	0.997	
Subreflector resistive	0.99977	0.99977	0.99977	
Subreflector surface rms	0.99986	0.99986	0.99986	
Waveguide resistive	0.99574	0.99574	0.99574	−0.01855 dB at 20 deg C
Waveguide voltage standing-wave ratio	0.991	0.991	0.991	
Quadripod blockage	0.922	0.922	0.922	
Total efficiency	0.8178	0.8250	0.8203	
Overall gain, dB	63.65	63.69	63.66	64.524 dB is 100 percent at 2.295 GHz

Computed G/T				
Element	G/T			Comments
	90 deg	45 deg	30 deg	
Computed G/T, dB/K	52.88	52.29	51.88	

Table 2. Gain and noise temperature budgets at 2.295 GHz for a 23.1-dBi horn.

Noise temperature budget				
Element	Noise temperature, K			Comments
	90 deg	45 deg	30 deg	
Cosmic background	2.7	2.7	2.7	Effective black body
Atmosphere	1.9	2.6	3.6	
Subreflector forward spillover	0	0	0	
Main reflector rear spillover	0.70	0.53	0.47	240 K, 0.29 percent
Main reflector resistive	0.08	0.08	0.08	
Main reflector gap leakage	0.1	0.1	0.1	
Subreflector resistive	0.07	0.07	0.07	
Quadripod scatter	2.3	3.8	4.2	
Subtotal	7.85	9.88	11.22	Noise at feed aperture
Modified subtotal	7.81	9.83	11.17	Noise at preamplifier input −0.01855 dB at 20 deg C
Waveguide resistive	1.25	1.25	1.25	
Coupler injection	0.093	0.093	0.093	
Low-noise amplifier	2.036	2.036	2.036	
Follow up	0.037	0.037	0.037	
Total noise temperature	11.23	13.25	14.59	

Gain budget				
Element	Efficiency			Comments
	90 deg	45 deg	30 deg	
P.O. computed subtotal	0.89467	0.90252	0.89738	Includes F1 field: Forward spill: 0.9716 Rear spill: 0.9971 Central blockage: 0.988
Main reflector resistive	0.99977	0.99977	0.99977	
Main reflector panel leakage	1	1	1	Calculated
Main reflector gap leakage	1	1	1	Calculated
Main reflector surface rms	0.997	0.997	0.997	
Subreflector resistive	0.99977	0.99977	0.99977	
Subreflector surface rms	0.99986	0.99986	0.99986	
Waveguide resistive	0.99574	0.99574	0.99574	−0.01855 dB at 20 deg C
Waveguide voltage standing-wave ratio	0.991	0.991	0.991	
Quadripod blockage	0.922	0.922	0.922	
Total efficiency	0.8110	0.8182	0.8135	
Overall gain, dB	63.61	63.65	63.63	64.524 dB is 100 percent at 2.295 GHz

Computed G/T				
Element	G/T			Comments
	90 deg	45 deg	30 deg	
Computed G/T, dB/K	53.11	52.43	51.99	

The second major design change was to replace the large matching groove in the throat section of the horn with a series of 10 slots tapered from approximately one-half wavelength to one-quarter wavelength in depth (Fig. 6). The tapered section provides a better match over a wider band than the single matching groove. The groove depths used in the tapered section are listed in Table 3. To accommodate the deeper slots of the taper at the input, the outside dimensions of the first horn section were enlarged, and the cold-water distribution hardware, which is not used, was removed.

Three minor design changes were made. First, the one-quarter wavelength slots are no longer constant throughout the entire horn. They are adjusted according to the horn radius to provide an effective electrical length of one-quarter wavelength [5]. Second, except for the input matching section, the slots

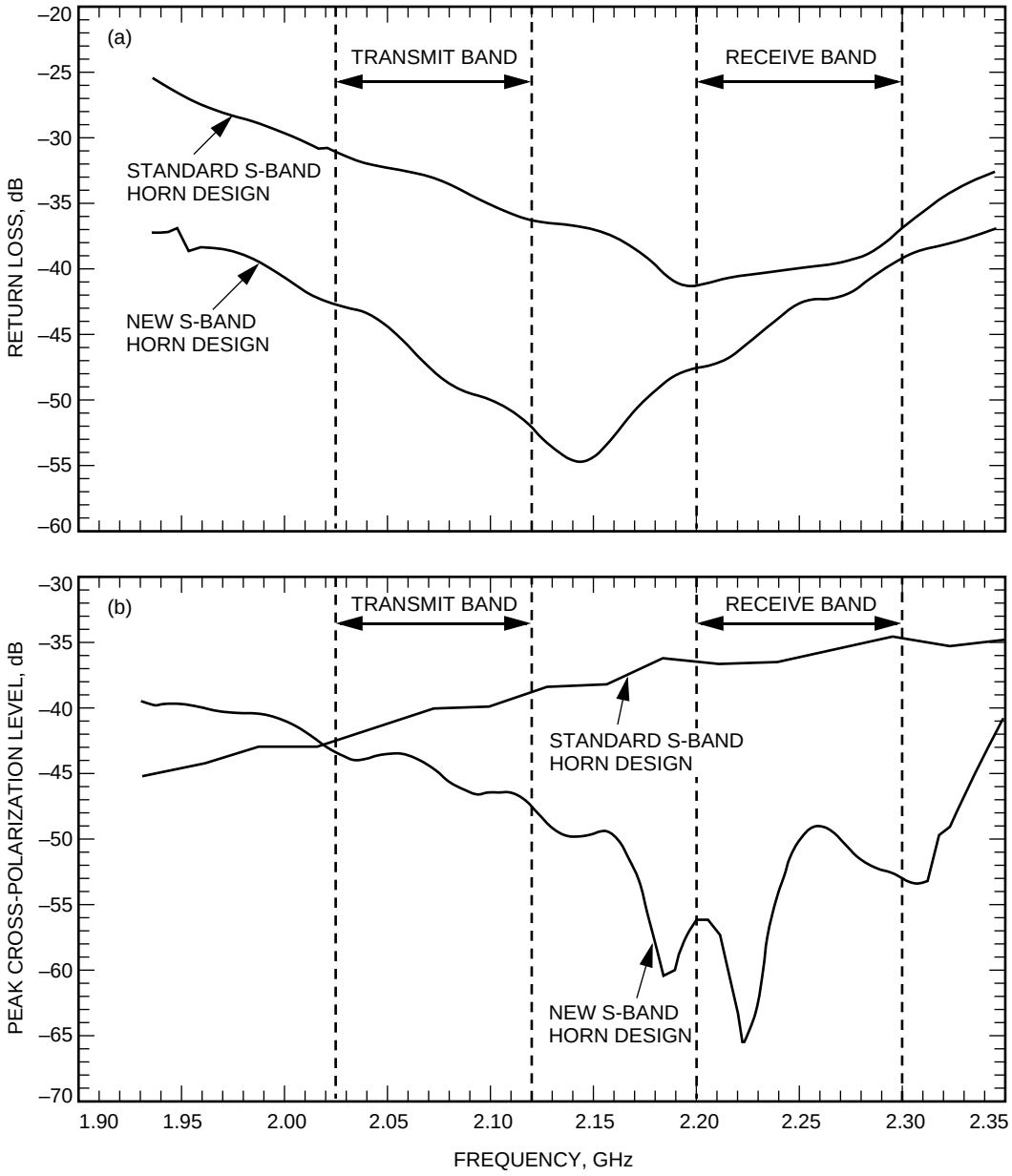

Fig. 4. Predicted performance of a standard S-band horn and the new S-band horn designs: (a) return loss and (b) peak cross-polarization levels.

are not as deep as those in the standard horn, making the outside dimensions of the horn slightly smaller. Reducing the depth of these slots improved the cross-polarization performance. Third, the new 22.5-dB horn is 1.7 cm longer than the standard 22.5-dB horn.

C. Noise Shield

Adding a noise shield around the edge of the main reflector dish was briefly considered. Physical optics programs were used to estimate the spillover past the main reflector dish with and without a noise shield. A 1-m shield would decrease the S-band noise temperature by 0.8 K at zenith, and a 2-m shield would provide a 1.1-K decrease at zenith. The cost of the noise shield was roughly estimated to be several hundred thousand dollars, which was deemed too expensive. No further investigation was made.

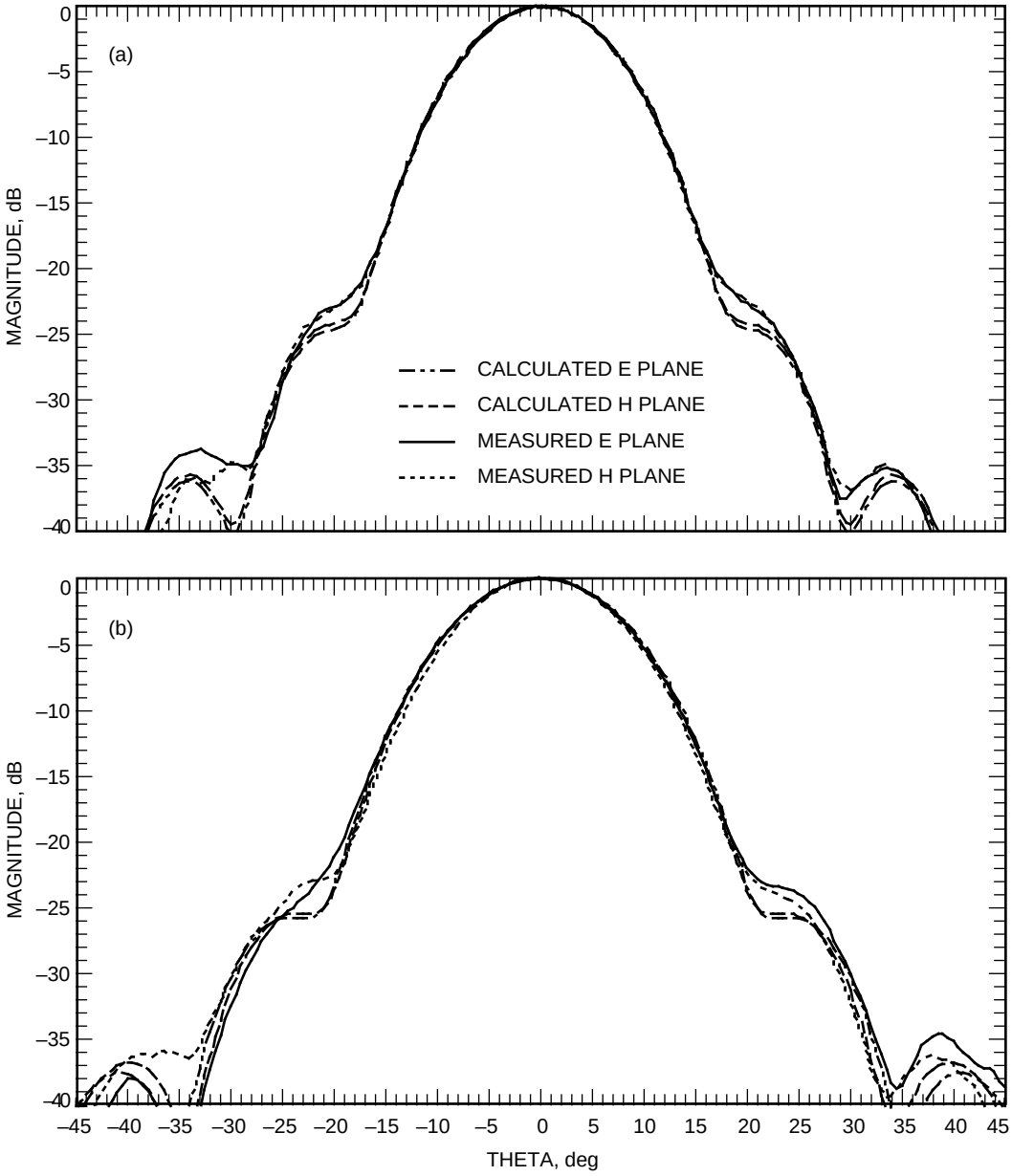

Fig. 5. Copolarization patterns of the new S-band horn at (a) 2.295 GHz and (b) 2.025 GHz.

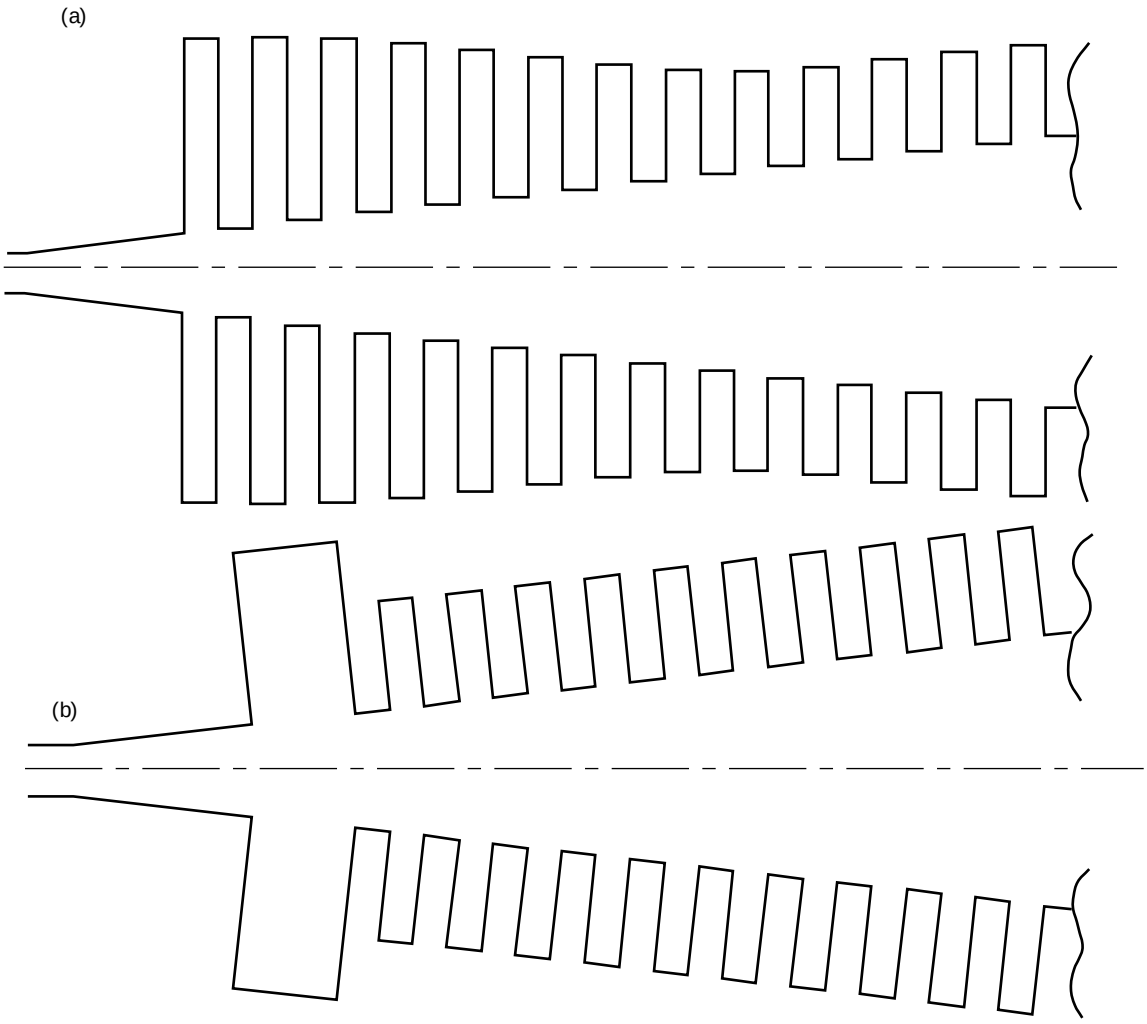

Fig. 6. Throat section of (a) the new S-band horn design and (b) a standard S-band horn.

IV. Preserving 22-GHz Performance

Installing the Ultracone horn in the F1 position and the 22-GHz radio-astronomy horn in the F2 position would create shadowing and interference problems between the two horns. By using a 23.1-dB S-band horn instead of the 22.5-dB horn, the shadowing and interference makes the 22-GHz system virtually unusable (Fig. 7). Options considered to avoid these problems were moving the S-band horn down along the feed axis, moving the 22-GHz horn up along the feed axis, moving the 22-GHz horn along the focus ring off F2, and adding a "stovepipe" extension to the top of the S-band horn to lower the feed and increase the horn gain. Moving the S-band horn along the focus ring, away from the 22-GHz horn, was not possible because of space constraints in the feed cone. In all cases, it was assumed that the S-band horn aperture flange would be trimmed to the minimum possible diameter.

A. Horn Relocation

The blockage of the 22-GHz horn by the S-band horn was estimated for several different positions of the two horns. The overall system performance was analyzed as the horns were moved off the feed focal

points. The analysis was completed using a combination of P.O. programs and the Geometric Theory of Diffraction (GTD) programs.

One possible way to reduce blockage of the 22-GHz horn was to move the S-band horn down along the feed axis. A computer analysis showed that the S-band performance is very insensitive to the horn location along the feed axis, but because of space constraints in the cone, this could not be done. The possibility of moving the 22-GHz horn up along the feed axis was examined. This defocuses the system by moving the phase center of the horn off the focal point of the main reflector and subreflector system. Part of this defocusing can be compensated for with subreflector displacement, if enough subreflector movement is available. Figure 8 shows the calculated gain loss from moving the horn, both with and without subreflector compensation, without considering losses due to blockage. With the 23.1-dB S-band horn, there is always significant blockage of the 22-GHz radiation pattern. With the 22.5-dB S-band horn, a 7.6-cm movement would prevent any appreciable blockage and would correspond to approximately a 0.2-dB loss in performance if subreflector compensation of 0.4 cm were used. If subreflector compensation could not be used, the loss from defocusing would be 0.6 dB.

Another approach investigated was to move the 22-GHz horn away from the S-band horn along the feed focal ring. Since the subreflector is designed to stop only at discrete locations along the focal ring, the horn would be defocused as it was moved from F2 towards F3 (Fig. 9). Figure 10 shows the computed gain loss from the horn movement, without considering losses due to blockage. Approximately 12.7 cm of movement, which would probably be the minimum movement possible to reduce the amount of blockage to acceptable levels, would cause about a 1.3-dB loss at 22 GHz due to defocusing, which is unacceptable.

Four specific cases were examined in more detail. The first case left the 22-GHz horn and the 22.5-dB S-band horn in their standard positions. The edge taper of the 22-GHz horn radiation pattern at the closest point of interference with the S-band horn was −11.5 dB. The radiation blocked by the S-band horn was integrated and found to be 2.2 percent of the total radiation, which would lead to approximately 0.1 dB of loss at 22 GHz. The second case was the same as the first, but with the 23.1-dB S-band horn. The pattern edge taper at the point of interference increased to −0.5 dB, which is totally unacceptable. The third case put the 22.5-dB S-band horn in its standard position with the 22-GHz horn moved 15.24 cm along the focal ring. The blockage in this case was insignificant. The fourth case was the same as the third, but with the 23.1-dB S-band horn. The pattern edge taper at the closest point of interference was −16.5 dB. The total power blocked was found by integration to be 0.8 percent, which would correspond to approximately a 0.035-dB loss.

Table 3. Taper section groove depths.

Slot number	Slot depth, cm
1	7.107
2	6.928
3	6.585
4	6.135
5	5.609
6	5.048
7	4.499
8	4.020
9	3.676
10	3.544

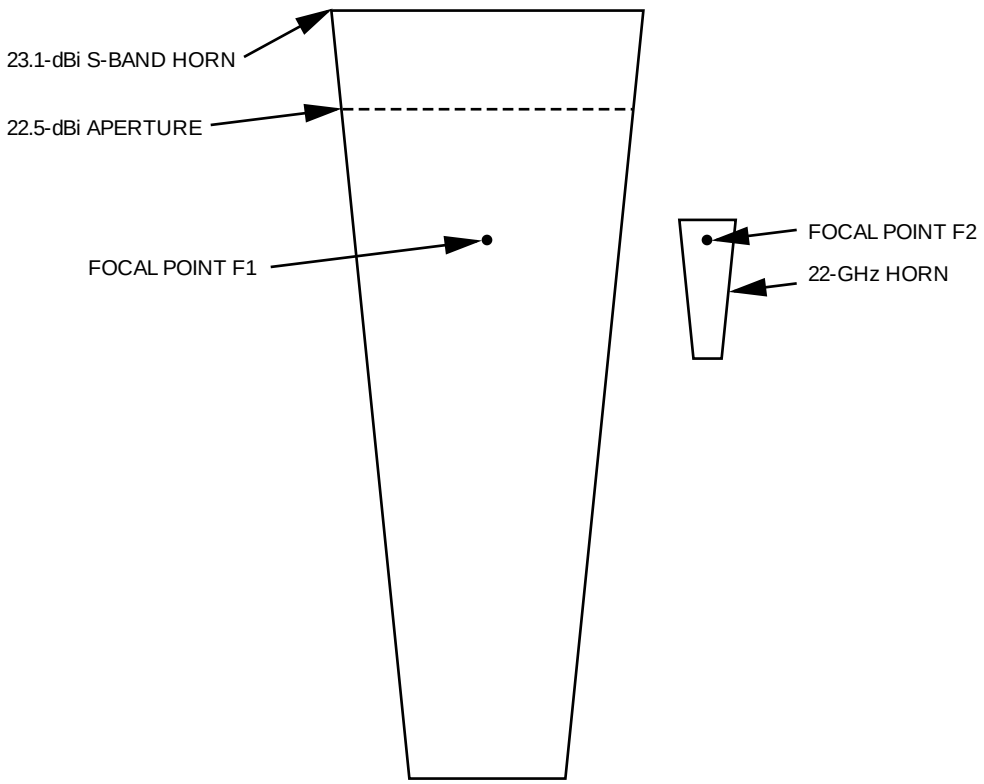

Fig. 7. Interference between the 23.1-dBi gain S-band horn, located at F1, and the 22-GHz horn, located at F2.

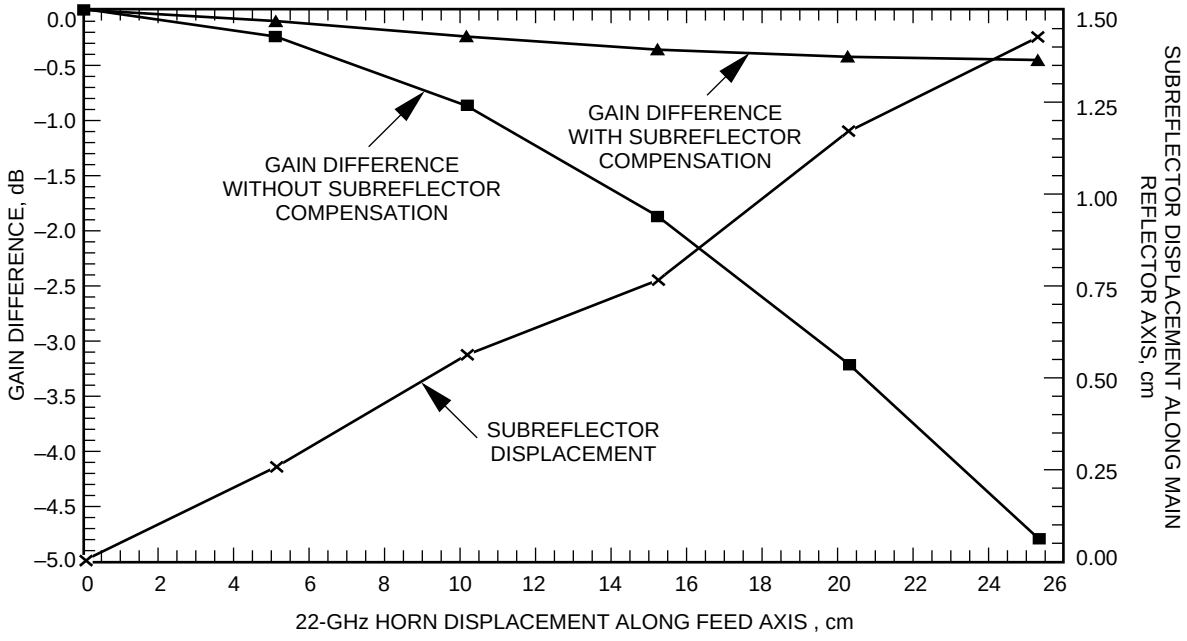

Fig. 8. Gain loss versus 22-GHz movement along the feed axis towards the subreflector, with and without subreflector compensation.

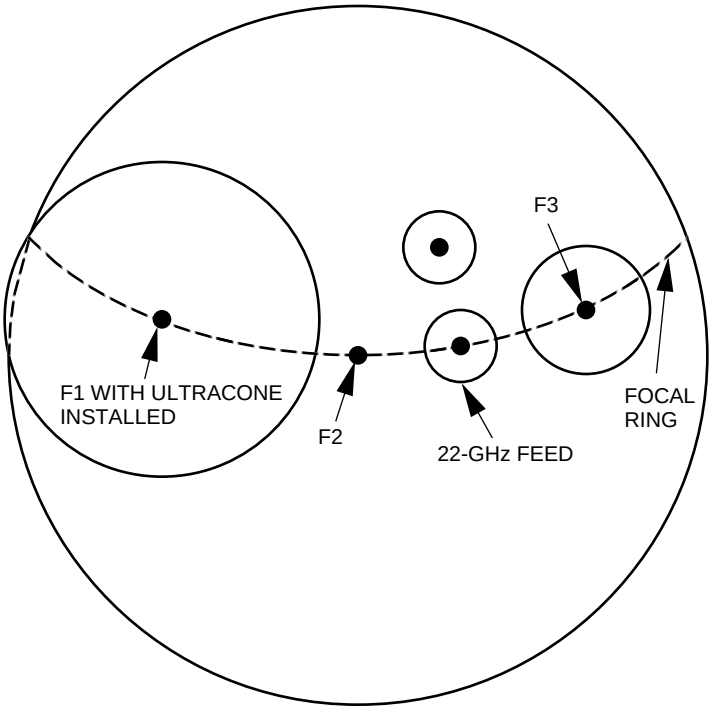

Fig. 9. Movement of the 22-GHz horn away from F2 towards F3.

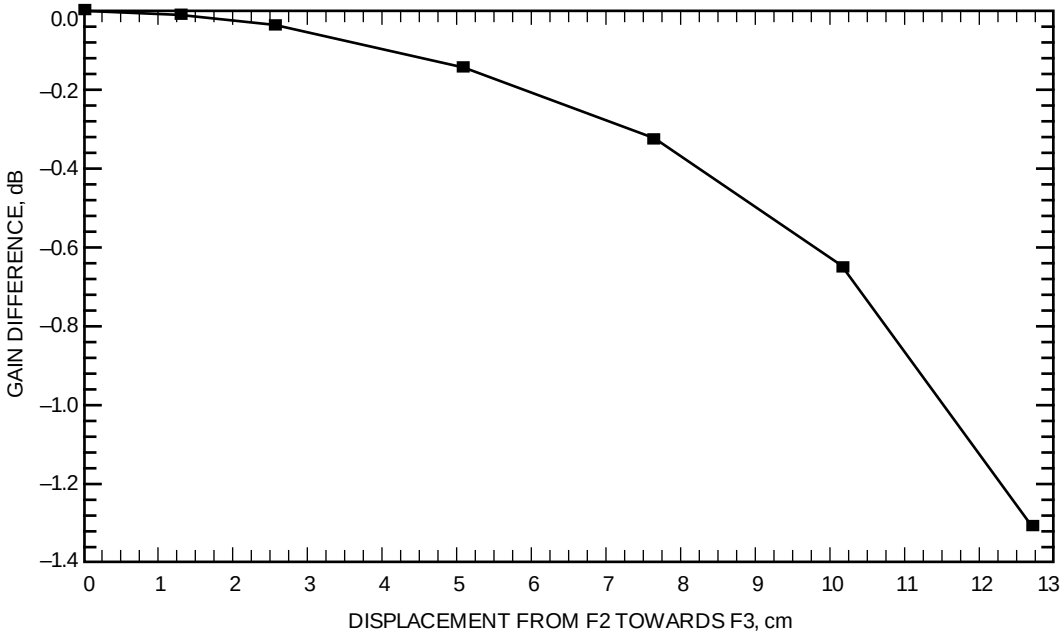

Fig. 10. Computed gain loss of the 22-GHz horn versus movement towards F3.

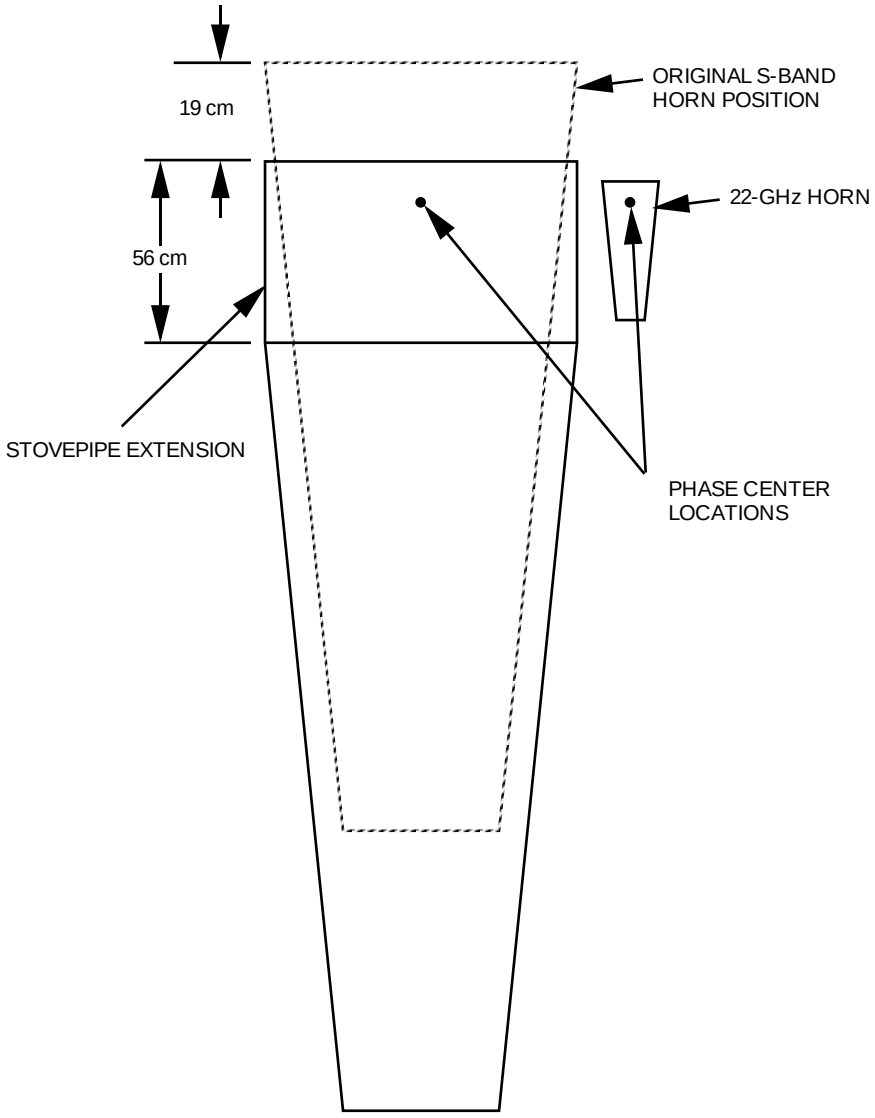

Fig. 11. Stovepipe configuration.

B. Stovepipe Design

One design alternative that was considered was a "stovepipe" extension [6] for the S-band horn. This design consists of adding a corrugated extension with no flare angle to the top of the horn. The extension moves the phase center of the feed horn to near the aperture of the horn and increases the gain of the horn. This would allow for a higher gain S-band horn while decreasing the shadowing of the 22-GHz horn by retaining the same aperture diameter and lowering the horn along the feed axis (Fig. 11). Using the data provided in [6], it was estimated that to move the aperture of the feed horn down 19 cm along the feed axis, an extension of 55.9 cm would be required to keep the phase center of the horn at the focal point. This would mean that the feed system would have to be moved down in the cone by 74.9 cm. This option was no longer considered when it was discovered that space in the feed cone did not allow the S-band horn to be lowered.

V. Conclusion

The RF study concluded that the S-band performance of the 70-m antenna could be improved by increasing the gain of the feed horn from 22.5 to 23.1 dB. A new, 23.1-dB horn was designed with better return loss and cross-polarization patterns than the standard JPL S-band horn. The Ultracone implementation will use the new feed horn in the F1 position of the host country's cone. The 22-GHz radio-astronomy horn that was originally in the F2 position must be relocated to reduce the blockage by the S-band horn to acceptable levels. Computer analysis showed that moving the 22-GHz horn 15.24 cm along the focal ring from F2 toward F3, as shown in Fig. 9, will reduce the blockage to 0.8 percent, which corresponds to a 0.035-dB loss.

The final design configuration chosen for implementation involved redesigning the subreflector positioner so that the subreflector can be moved to any angle. This allows the system to focus on any point on the focal ring instead of only three discrete points in each feed cone. The 22-GHz feed will be moved along the focal ring by 15.24 cm, and the subreflector will be repositioned so that no losses due to defocusing will be incurred.

Acknowledgments

The authors thank D. Trowbridge and S. Petty for providing data for gain and noise budget estimates, H. Reilly and R. Cirillo for the feed horn antenna measurements, O. Casanova for providing valuable information and support, and P. Stanton for reviewing this article. The Cray supercomputer used in this investigation was provided by funding from the NASA Offices of Mission to Planet Earth, Aeronautics, and Space Science.

References

[1] D. Hoppe, "Scattering Matrix Program for Circular Waveguide Junctions," *Cosmic Software Catalog*, 1987 edition, NASA-CR-179669, NTO-17245, NASA's Computer Software Management and Information Center, Athens, Georgia, 1987.

[2] G. L. James, "Analysis and Design of TE_{11}-to-HE_{11} Corrugated Cylindrical Waveguide Mode Converters," *IEEE Transactions on Microwave Theory and Techniques*, vol. MTT-29, no. 10, pp. 1059–1066, October 1981.

[3] S. Silver, *Microwave Antenna Theory and Design*, New York: McGraw-Hill, pp. 336–337, 1949.

[4] P. Clarricoats and A. Olver, *Corrugated Horns for Microwave Antennas*, London: Peter Peregrinus Ltd., pp. 120–122, 1984.

[5] B. Thomas, G. James, and K. Greene, "Design of Wide-Band Corrugated Conical Horns for Cassegrain Antennas," *IEEE Transactions on Antennas and Propagation*, vol. AP-34, no. 6, pp. 750–757, June 1986.

[6] F. Manshadi and R. Hartop, "Compound-Taper Feedhorn for NASA 70-m Antennas," *IEEE Transactions on Antennas and Propagation*, vol. 36, no. 9, pp. 1213–1216, September 1988.